Proc. Natl. Acad. Sci. USA
Vol. 93, pp. 12304–12308, October 1996
Cell Biology

Cytoplasm-to-vacuole targeting and autophagy employ the same machinery to deliver proteins to the yeast vacuole

(aminopeptidase I/protein targeting/vacuolar ATPase)

SIDNEY V. SCOTT*, ANN HEFNER-GRAVINK*, KEVIN A. MORANO*, TAKESHI NODA†, YOSHINORI OHSUMI†, AND DANIEL J. KLIONSKY*

*Section of Microbiology, University of California, Davis, CA 95616; and †Department of Cell Biology, National Institute for Basic Biology, Myodaiji-cho, Okazaki 444, Japan

Communicated by William T. Wickner, Dartmouth Medical School, Hanover, NH, August 7, 1996 (received for review June 17, 1996)

ABSTRACT **The vacuolar protein aminopeptidase I (API) uses a novel cytoplasm-to-vacuole targeting (Cvt) pathway. Complementation analysis of yeast mutants defective for cytoplasm-to-vacuole protein targeting (*cvt*) and autophagy (*apg*) revealed seven overlapping complementation groups between these two sets of mutants. In addition, all 14 *apg* complementation groups are defective in the delivery of API to the vacuole. Similarly, the majority of nonoverlapping *cvt* complementation groups appear to be at least partially defective in autophagy. Kinetic analyses of protein delivery rates indicate that autophagic protein uptake is induced by nitrogen starvation, whereas Cvt is a constitutive biosynthetic pathway. However, the machinery governing Cvt is affected by nitrogen starvation as targeting defects resulting from API overexpression can be rescued by induction of autophagy.**

The vacuole/lysosome is the major hydrolytic compartment of the cell and as such is central to survival during nitrogen starvation (1). When cells sense nitrogen starvation, cytoplasmic proteins and organelles are packaged nonselectively into autophagosomes, which are then targeted to the vacuole for degradation and turnover of their constituent components by resident hydrolases (2, 3). In this manner, amino acids as well as nucleic acids can be recycled to enable stress survival. In yeast, this autophagic process has been studied primarily through microscopic analysis. During autophagy, large double-membraned vesicles (500 nm) nonselectively surround cytoplasmic proteins and organelles (2, 4). On delivery to the vacuole, the outermost membrane is proposed to fuse to the vacuolar membrane, resulting in the delivery of a still intact vesicle (autophagic body) into the vacuolar lumen (2, 5). These autophagic bodies are then degraded in a subsequent step that depends on proteinase B (4). Although two collections of autophagy mutants have been identified (6, 7), the molecular details of this process have not yet been elucidated.

The resident hydrolases that mediate the digestive capacity of the vacuole are delivered to this organelle by two distinctly different protein transport pathways. The majority of vacuolar proteins are targeted through the secretory pathway (reviewed in refs. 8 and 9), whereas at least one vacuolar protein, aminopeptidase I (API) (10), uses the cytoplasm-to-vacuole targeting (Cvt) pathway. In mammalian cells, decreasing lumenal pH through the endocytic compartments is proposed to mediate the receptor/ligand dissociation reactions required for correct sorting through these compartments (11). Early evidence suggests that the same mechanism may mediate sorting in yeast as well; one important feature of the vacuolar membrane is the presence of a vacuolar ATPase (V-ATPase), which uses ATP to transport protons into the lumen. Maintenance of the resulting ΔpH is essential not only for optimal activity of many vacuolar proteases but also for efficient delivery of soluble vacuolar proteins by the secretory (12–14) and Cvt (15) pathways.

The vacuolar hydrolase API is synthesized as a cytosolic precursor containing an N-terminal targeting signal that directs it to the vacuole (16). Characterization of Cvt using API as a marker protein revealed that transport by this pathway has a half-time for vacuolar delivery of 30–45 min (10), uses both an ATPase and a GTPase, and is inhibited at temperatures below 15°C (15). Seventeen complementation groups of yeast mutants that fail to mature API have been identified (called *cvt* for cytoplasm-to-vacuole targeting) (17, 18). The majority of these mutants are not defective in delivery of vacuolar proteins by the secretory pathway, indicating that these two mechanisms of vacuolar delivery constitute biochemically distinct pathways. Three *cvt* complementation groups are, however, allelic to previously identified (6) autophagy (*aut*) mutants, suggesting that there may be some commonality between Cvt and autophagy (17).

To further characterize the connection between Cvt and autophagy, we analyzed a second group of autophagy mutants (*apg*) (7) for genetic overlap with *cvt* mutants and defects in API targeting. In addition, we used a new biochemical marker for autophagic protein uptake (19) to simultaneously analyze protein trafficking by these two pathways *in vivo*. We found that, although there is significant genetic overlap between these two pathways, they are regulated differently; API import is constitutive and not dependent on nutrient conditions, whereas delivery of proteins to the vacuole by autophagy can only be detected under starvation conditions and occurs with a much longer half-time.

METHODS

Yeast Strains and Media. The *Saccharomyces cerevisiae* strains used in this study were SEY6210, *MATα leu2-3,112 ura3-52 his3-Δ200 trp1-Δ901 lys2-801 suc2-Δ9 GAL* (20), and SEY6211, *MATa leu2-3,112 ura3-52 his3-Δ200 trp1-Δ901 lys2-801 suc2-Δ9 GAL* (20). *cvt* strains 1–17 were derived from SEY6210 and SEY6211 (17, 18). *apg* strains were derived from X2180-1A, *MATa SUC2 mal mel gal2 CUP1* (7, 21); TN121, *MATa leu2-3, 112 trp1 ura3-52 pho8::pho8Δ60 pho13::URA3* (19); and TN124, *MATa leu2-3, 112 trp1 ura3-52 pho8::pho8Δ60 pho13::LEU2* (19). KMY4 was obtained by crossing TN121 to KMY1004 (*MATα leu2-3, 112 ura3-52 his3-Δ200 trp1-Δ901 lys2-801 suc2-Δ9 GAL vma4::LEU2*) (14), sporulating and selecting a haploid that was *Δvma4* and

The publication costs of this article were defrayed in part by page charge payment. This article must therefore be hereby marked "*advertisement*" in accordance with 18 U.S.C. §1734 solely to indicate this fact.

Abbreviations: API, aminopeptidase I; Cvt, cytoplasm-to-vacuole targeting; SMD, synthetic minimal medium containing 2% glucose, essential amino acids, and ammonium sulfate; SD-N, synthetic minimal medium without ammonium sulfate but containing 2% glucose; V-ATPase, vacuolar ATPase; YPD, 1% yeast extract, 2% peptone, and 2% glucose; prAPI, precursor-sized API.

contained Pho8Δ60p. The plasmid pRC1 (2 μ *APEI*) has been previously described (10). The following media were used: synthetic minimal medium containing 2% glucose, essential amino acids, and ammonium sulfate (SMD); synthetic minimal medium without amino acids or ammonium sulfate but containing 2% glucose (SD-N); and 1% yeast extract, 2% peptone, and 2% glucose (YPD). Δ*vma4* strains were maintained in medium buffered with 50 mM Mes/50 mM Mops, pH 5.5.

Materials. Antiserum against API was as described (10). Antiserum to Pho8p was produced using two previously described peptides corresponding to amino acid residues 222–244 (AP22) and 281–301 (AP24) of the *PHO8* gene that were conjugated separately to keyhole limpet hemocyanin (22). Equal amounts (0.5 mg) of the conjugated peptides were mixed with Freund's complete adjuvant and injected into a male New Zealand White rabbit. A secondary immunization (100 μg) after 4 weeks was followed by antiserum collection at 1-month intervals for a period of 12 months. Other materials were of reagent grade.

Nitrogen Starvation Experiments. To examine cell survival under poor nutrient conditions, cells grown to exponential phase in YPD were harvested, washed twice with and resuspended in SD-N to a final concentration of 1 OD_{600} unit/ml, and incubated at 30°C. Aliquots taken at days 0–6 were spread on YPD plates to determine cell viability. Colonies from three replicates of each time point were counted after 2 days growth at 30°C.

Pulse–Chase Analysis. Yeast strains were grown to 1 OD_{600} unit/ml in SMD and pulse-labeled for the times indicated (18). Cold cysteine and methionine were added to 20 μM and 10 μM, respectively. The labeled cells were harvested and resuspended at 1 OD_{600} unit/ml in either SMD or SD-N and chased at 30°C for the time indicated. In experiments in which Δ*vma4* strains were used, SMD and SD-N were buffered with 50 mM Mes/50 mM Mops, pH 5.5. At each time point, whole cells were precipitated with 10% trichloroacetic acid and washed once with acetone, and the dried cell pellet was resuspended in 100 μl Mes-urea resuspension buffer (50 mM sodium phosphate/25 mM Mes, pH 7.0/1% SDS/0.5% 2-mercaptoethanol/1 mM sodium azide). Glass beads were added, and the cells were lysed by mixing for 5 min at full speed on a multi-mixer (Tomy, Palo Alto, CA; model MT-360). The resulting supernatants were subjected to double immunoprecipitation reactions with the indicated antibodies as described (10). Immunoprecipitated proteins were resolved by SDS/PAGE and detected and quantitated using either a Fuji FUJIX BAS1000 Bioimaging analyzer or a Molecular Dynamics STORM PhosphorImager as indicated. Data are expressed as the percent of total protein recovered that is mature-sized.

Other Methods. Complementation analysis was essentially as described (23) with modifications (17). Western blotting was as described (18).

RESULTS

Genetic and Phenotypic Overlap Between *cvt* and *apg* Complementation Groups. Because both autophagy and Cvt result in the transport of full-length proteins from the cytosol to the vacuole, we crossed representative *cvt* alleles to the *apg* mutant collection. The resulting diploids were screened by Western blot analysis for accumulation of precursor-sized API (prAPI). This diagnostic test, based on the pretense that mutants in API delivery will accumulate the precursor-sized protein, was used previously for the isolation of the *cvt* mutants (18). Noncomplementing mutants were identified as diploids that accumulate prAPI. Six of the *cvt* mutants failed to complement *apg* mutants (Table 1). In addition, the remaining eight *apg* alleles were screened by Western blotting for accumulation of prAPI, and all were found to be severely defective in API maturation (data not shown).

Table 1. Genetic overlap between *cvt* and *apg* strains

cvt	*apg*
cvt2	*apg7*
cvt5	*apg8*
cvt7	*apg9*
cvt10	*apg1*
cvt11	*apg15*
cvt12	*apg14*

To determine the defect in the API import pathway caused by the *apg* mutations, subcellular fractionation experiments were performed. In *cvt* mutants, accumulated prAPI is in the cytosolic fraction and is protease-sensitive (17, 18). The same fractionation pattern was observed for the nonoverlapping *apg* mutants (data not shown), with the exception of *apg2*. A fraction of prAPI in this strain localized to the organellar pellet fraction, where it was also sensitive to digestion by added protease (data not shown). This fractionation pattern suggests that some prAPI is associated with the surface of a vesicle or organelle in *apg2*. The fact that prAPI is protease-sensitive in all *apg* strains indicates that vacuolar delivery is blocked in these mutants.

Yeast mutants that are defective for autophagy are unable to survive nitrogen starvation (7). To investigate whether *cvt* alleles that are not allelic to known autophagy mutants share this phenotype, nitrogen starvation experiments were performed. Haploid cells were grown in YPD, diluted into nitrogen starvation medium (SD-N), and plated daily onto YPD plates. Wild-type cells survived this regime without a decrease in viability, whereas *cvt10* (*apg1*) died after only 3 days in SD-N (Fig. 1). The mutants *cvt3* and *cvt6* had intermediate phenotypes; *cvt6* died after 4 days, and the viability of *cvt3* began to decline after 5–6 days of nitrogen starvation (Fig. 1). These results suggest that these two *cvt* mutants, which do not overlap with any of the characterized autophagy mutants, may also have some defect in autophagy but may be less severely affected than classic autophagy mutants such as *apg1*. The *cvt* strains that have defects in vacuolar protein sorting through the secretory pathway were not subjected to this analysis.

Pulse–Chase Analysis of API Maturation and Autophagic Protein Delivery. Recently, a biochemical assay for autophagic protein uptake was developed. This assay uses a modified form of vacuolar alkaline phosphatase in which the first 60 N-

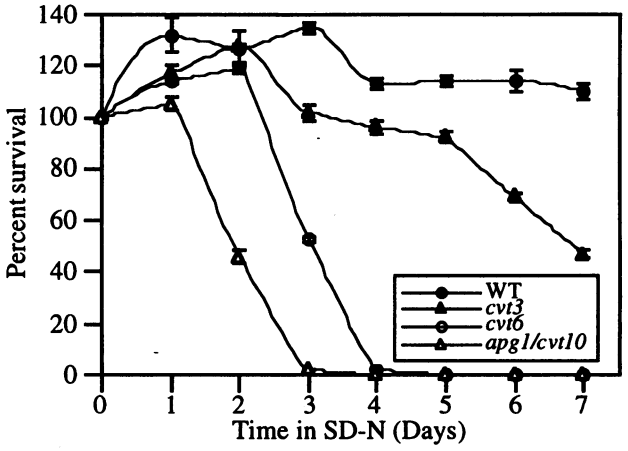

FIG. 1. Mutants defective in Cvt exhibit different abilities to survive nitrogen starvation. Strains were grown in YPD to an OD_{600} of 1.0–1.6 and then transferred to SD-N. At the indicated times, aliquots of cells were diluted and plated on YPD. Percent survival was determined by counting the number of surviving colonies from triplicate platings and dividing the number of colonies at each time point by the average number of colonies obtained at day 0.

terminal amino acids have been deleted (Pho8Δ60p). Because this region contains the membrane-spanning domain that acts as a signal sequence for translocation into the endoplasmic reticulum (22), Pho8Δ60p does not enter the secretory pathway and remains in the cytosol. However, Pho8Δ60p does contain a cleavage site for proteinase B so that vacuolar delivery by autophagy can be monitored by the appearance of a lower molecular weight product (20).

To examine the kinetics of API transport and autophagy simultaneously, pulse–chase experiments were performed using the yeast strain TN124, in which the *PHO8Δ60* replaces the genomic copy of *PHO8*. Yeast were grown and pulse-labeled in SMD media and subjected to chase either in SMD or in nitrogen starvation media (SD-N). Samples collected at the chase times indicated were subjected to immunoprecipitation with both anti-API and anti-Pho8p antiserum. The maturation kinetics of API were nearly identical in both chase conditions (Fig. 2*B*), indicating that the kinetics of API transport are not affected by nitrogen starvation. Over the same time course, Pho8Δ60p was only delivered to the vacuole when autophagy was induced by nitrogen starvation (Fig. 2*A*). Under these conditions, mature Pho8Δ60p was detected after 2 hr of chase. Over the time course analyzed, 27% of the newly synthesized

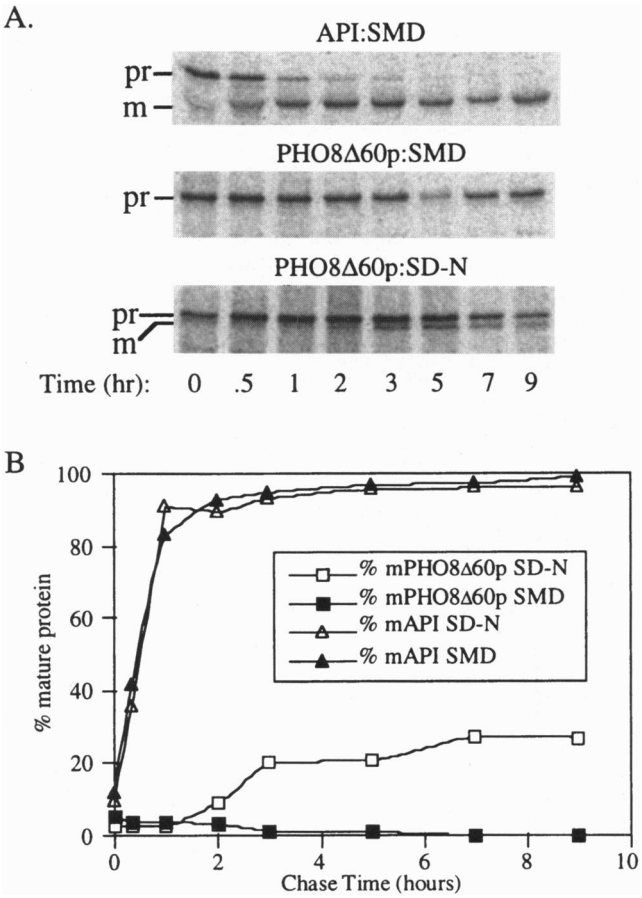

FIG. 2. Kinetics of API and Pho8Δ60p delivery. TN124 was pulse-labeled for 10 min, pelleted, and resuspended in either SMD (closed symbols) or SD-N (open symbols). Aliquots were collected for immunoprecipitation with antibodies against API and Pho8p at the indicated times. The resulting proteins were resolved by SDS/PAGE and detected and quantified using a Fuji BAS1000 phosphorimager. The locations of the precursor (pr) and mature (m) forms of the polypeptides are indicated. (*A Top*) API pulse–chase in SMD. Results with SD-N were essentially identical to those shown for SMD. (*Middle*) Pho8Δ60p pulse–chase in SMD. (*Bottom*) Pho8Δ60p in SD-N. (*B*) Quantitation of experiments in *A*, including data from the API chase in SD-N.

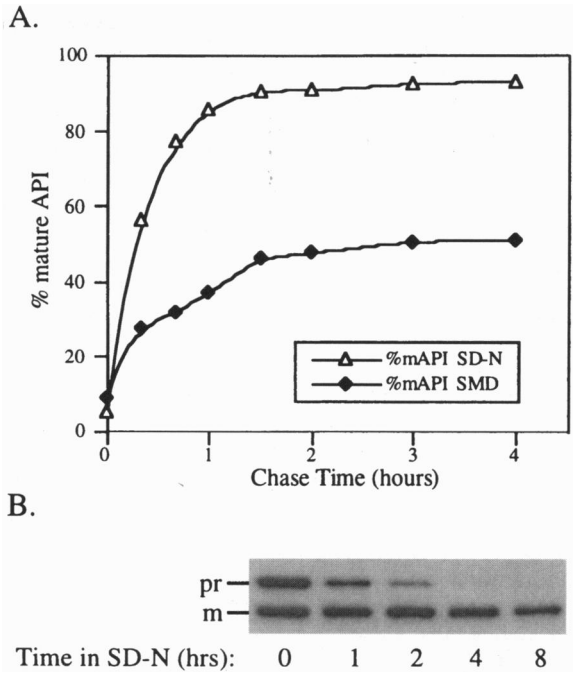

FIG. 3. (*A*) Nitrogen starvation prevents prAPI accumulation from an overexpression plasmid. Yeast strain SEY6210 containing the 2μ plasmid pRC1 was pulse-labeled for 6 min in SMD, pelleted, and resuspended in either SMD or SD-N. Aliquots were collected for immunoprecipitation at the indicated times. After immunoprecipitation with API antibodies, the samples were resolved by SDS/PAGE and detected and quantitated with a Molecular Dynamics STORM PhosphorImager. (*B*) SEY6210 cells containing the 2μ plasmid pRC1 were grown overnight in SMD to an OD_{600} of 1, harvested, washed in distilled water, resuspended at 1 OD_{600} unit/ml in SD-N, and incubated at 30°C. At the times indicated, cell aliquots were precipitated with trichloroacetic acid and subjected to Western blotting with anti-API antibody.

Pho8Δ60p was delivered to the vacuole. If the rate of autophagy is extrapolated from the kinetics of maturation between the 1 and 7 hr time points, the rate of vacuolar delivery by autophagy was about 4%/hr, significantly slower than the rate of API delivery. Because API transport is rapid compared with autophagy, pulse–chase analysis of API maturation was performed under nitrogen starvation conditions to determine if preinduction of autophagy altered the kinetics of API import. Cells were incubated in SD-N for 2 hr before labeling to induce nitrogen starvation. Pulse-chase analysis of autophagy-induced cells was then performed in SD-N. This treatment had no effect on the kinetics of API maturation, although the relative synthesis level of API was induced about 19-fold over cells labeled in SMD (data not shown).

Nitrogen Starvation Prevents prAPI Accumulation Caused by Overexpression. When API is expressed from a 2μ plasmid that causes approximately a 20- to 30-fold induction in API synthesis, 40–50% of the API present in the cell remains as the precursor form in the cytosol, suggesting saturation of the import machinery (10). To examine whether nitrogen starvation increases the machinery available for API transport, cells harboring a 2μ API-bearing plasmid were pulse-labeled in SMD and subjected to a chase in either SMD or SD-N. As expected, when cells containing the overexpression plasmid were subjected to a chase in SMD, transport plateaued after only 50% of the newly synthesized API precursor reached the vacuole (Fig. 3*A*). However, when an identically labeled aliquot of cells was shifted to the nitrogen starvation medium for the chase reaction, there was an immediate stimulation of transport, and the prAPI was nearly completely targeted to the vacuole (Fig. 3*A*). These data suggest that nitrogen starvation

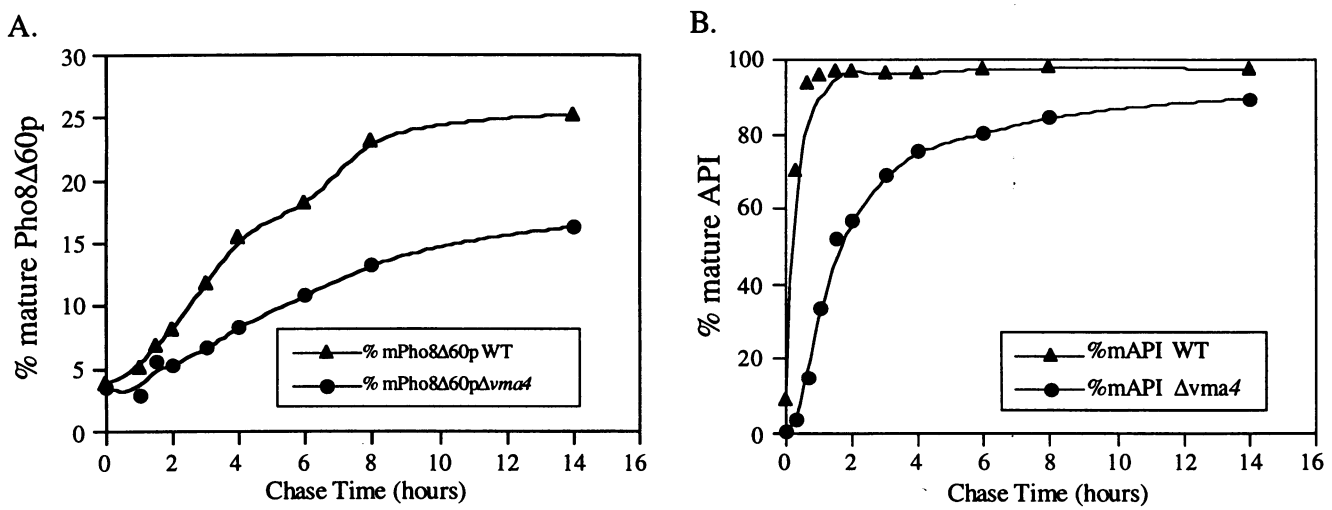

FIG. 4. Transport kinetics in a Δ*vma4* strain. KMY4 (Δ*vma4*) and TN121 (WT) cells were pulse-labeled for 6 min, collected by centrifugation, and resuspended in SD-N. At the times indicated, an aliquot was collected for immunoprecipitation. After immunoprecipitation with API and Pho8p antibodies, the samples were resolved by SDS/PAGE and detected and quantitated with a Molecular Dynamics STORM PhosphorImager. (*A*) Percent mature Pho8Δ60p. (*B*) Percent mature API.

causes a rapid increase in the availability of API transport machinery. To investigate whether nitrogen starvation could rescue accumulated prAPI from cells containing API on the 2μ plasmid, a Western blot experiment was performed. Yeast were grown overnight in the nitrogen containing medium SMD to an OD_{600} of 1. They were then harvested, washed in distilled water, and resuspended in SD-N at an OD_{600} of 1. Equal aliquots of cells were collected at the indicated times after switching to SD-N, and protein extracts were prepared and subjected to immunoblot analysis. At time 0, after growth in SMD, about 50% of the API present was precursor-sized, suggesting that the Cvt machinery was saturated (Fig. 3*B*). After 1 hr of nitrogen starvation, a considerable portion of this accumulated precursor disappeared, suggesting rapid delivery to the vacuole on induction of autophagy. This transport event was both complete and rapid, indicating that it is a selective process.

V-ATPase Is Required for Efficient Transport. To provide a further comparison of the mechanistic requirements of autophagy and Cvt, we analyzed the effect of deletion of one of the peripheral subunits of the V-ATPase on the kinetics of transport by these pathways. The Δ*vma4* strain KMY1004 was crossed to TN121 to create the yeast strain KMY4, which contains both the *VMA4* deletion and has *PHO8Δ60* integrated into the genome, replacing *PHO8*. Pulse–chase experiments were then performed to assess the rate of transport of API and Pho8Δ60p in this strain. The maturation kinetics of both API and Pho8Δ60p were substantially delayed by the ATPase defect (Fig. 4), suggesting a role for the vacuolar ΔpH in delivery by both pathways.

DISCUSSION

Genetic analysis of two classes of yeast mutants, *cvt* and *apg*, revealed that these two pathways apparently use largely the same group of molecular components. Further, phenotypic analysis of these mutants revealed that all 14 *apg* complementation groups are defective for API targeting (Fig. 1; data not shown). Sensitivity to nitrogen starvation suggests that the *cvt* mutants examined have at least a modest defect in autophagy (Fig. 2). This is surprising in that these two groups of mutants were isolated by seemingly distinct screens; the *cvt* mutants were isolated on the basis of prAPI accumulation (17, 18), whereas the *apg* mutants were screened for defects in vesicle accumulation after nitrogen starvation (7).

In vivo pulse–chase experiments further suggest a relationship between these two pathways. Although the maximal rate of API transport appears unaffected by nitrogen starvation (Fig. 2), experiments in which API is overexpressed suggest that an increase in the capacity for API transport correlates with induction of autophagy (Fig. 3). This increase in capacity could be due to mobilization of transport machinery that provides for the specific targeting of biosynthetic proteins such as API as well as an increase in the nonselective transport of cytoplasmic proteins and organelles destined for turnover in the vacuole. The fact that nitrogen starvation induces both the synthesis and the transport capacity of API may indicate either a particular role for this polypeptide in survival during nutrient stress or a general up-regulation of vacuolar capacity under these conditions.

A further similarity between Cvt and autophagy is that both transport pathways experience a kinetic delay based on processing of prAPI and Pho8Δ60p in strains in which the V-ATPase is defective (Fig. 4). For API transport, this inhibition has been shown to be a primary effect of V-ATPase disruption. When the vacuolar ΔpH is collapsed with chemical agents, such as the specific V-ATPase inhibitor bafilomycin A_1, API delivery is quickly impaired (15). That the targeting defect exhibited in Δ*vma4* strains is manifested as a kinetic block suggests that it is the vacuolar ΔpH which is involved in targeting rather than the pumping action of the V-ATPase itself. Even in an ATPase mutant, the vacuole is acidified to a certain degree by fluid phase endocytosis (24). This mechanism probably compensates for the V-ATPase mutation and allows for autophagic delivery and API targeting to continue at reduced rates. Alternatively, slower kinetics for maturation of the marker proteins used in this study may reflect reduced activity of the vacuolar hydrolases as a result of the increased lumenal pH. This could result in increased stability of the autophagosomes and/or decreased processing capacity of the organelle. We consider the latter possibility unlikely, however, because *vma* null mutants retain substantial proteolytic activity (13).

Kinetic experiments also revealed two primary differences between these two pathways. First, measurable delivery of proteins to the vacuole by autophagy requires induction by nutrient deprivation, whereas API delivery is efficient both in the presence and absence of autophagy induction (Fig. 2). This finding suggests that if API is delivered to the vacuole by autophagosomes, there must be a low constitutive level of

these vesicles that is normally sufficient for API delivery. Second, API is quantitatively delivered to the vacuole, whereas delivery of Pho8Δ60p by autophagy reaches equilibrium at about 30% mature protein. In addition, the rate of API delivery is more than 20 times faster than even the induced rate of autophagy (Fig. 2). These results indicate that API transport differs from autophagy in that it is a selective process. The API proregion is essential for API targeting and specifically for the membrane binding event of the targeting process (16). The role of the proregion could be to direct API to bind either to a specific API receptor on or near the site of autophagosome formation, or to bind directly to one of the constitutive components of autophagosomes. A second possible model is that API first binds directly to the surface of the vacuole itself, and its subsequent entry into the vacuole is triggered by delivery of autophagosomes. Further analysis of the mechanism of API import will likely provide a greater understanding of the autophagic process.

We thank Tanya Harding for her assistance with the genetic analysis of the *cvt* mutants and for helpful discussion and comments. This work was supported by a National Institutes of Health Molecular and Cellular Biology Training Grant to A.H.-G. and by Public Health Service Grant GM53396 from the National Institutes of Heath to D.J.K.

1. Teichert, U., Mechler, B., Muller, H. & Wolf, D. H. (1989) *J. Biol. Chem.* **264,** 16037–16045.
2. Baba, M., Takeshige, K., Baba, N. & Ohsumi, Y. (1994) *J. Cell Biol.* **124,** 903–913.
3. Klionsky, D. J., Herman, P. K. & Emr, S. D. (1990) *Microbiol. Rev.* **54,** 266–292.
4. Takeshige, K., Baba, M., Tsuboi, S., Noda, T. & Ohsumi, Y. (1992) *J. Cell Biol.* **119,** 301–311.
5. Baba, M., Osumi, M. & Ohsumi, Y. (1995) *Cell Struct. Funct.* **20,** 465–471.
6. Thumm, M., Egner, R., Koch, M., Schlumpberger, M., Straub, M., Veenhuis, M. & Wolf, D. H. (1994) *FEBS Lett.* **349,** 275–280.
7. Tsukada, M. & Ohsumi, Y. (1993) *FEBS Lett.* **333,** 169–174.
8. Stack, J. H., Horazdovsky, B. & Emr, S. D. (1995) *Annu. Rev. Cell Dev. Biol.* **11,** 1–33.
9. Conibear, E. & Stevens, T. H. (1995) *Cell* **83,** 513–516.
10. Klionsky, D. J., Cueva, R. & Yaver, D. S. (1992) *J. Cell Biol.* **119,** 287–299.
11. van Weert, A. W., Dunn, K. W., Gueze, H. J., Maxfield, F. R. & Stoorvogel, W. (1995) *J. Cell Biol.* **130,** 821–834.
12. Umemoto, N., Yoshihisa, T., Hirata, R. & Anraku, Y. (1990) *J. Biol. Chem.* **265,** 18447–18453.
13. Klionsky, D. J., Nelson, H. & Nelson, N. (1992) *J. Biol. Chem.* **267,** 3416–3422.
14. Morano, K. A. & Klionsky, D. J. (1994) *J. Cell Sci.* **107,** 2813–2824.
15. Scott, S. V. & Klionsky, D. J. (1995) *J. Cell Biol.* **131,** 1727–1735.
16. Oda, M. N., Scott, S. V., Hefner-Gravink, A., Caffarelli, A. D. & Klionsky, D. J. (1996) *J. Cell Biol.* **132,** 999-1010.
17. Harding, T. M., Hefner-Gravink, A., Thumm, M. & Klionsky, D. J. (1996) *J. Biol. Chem.* **30,** 17621–17624.
18. Harding, T. M., Morano, K. A., Scott, S. V. & Klionsky, D. J. (1995) *J. Cell Biol.* **131,** 591–602.
19. Noda, T., Matsuura, A., Wada, Y. & Ohsumi, Y. (1995) *Biochem. Biophys. Res. Commun.* **210,** 126–132.
20. Robinson, J. S., Klionsky, D. J., Banta, L. M. & Emr, S. D. (1988) *Mol. Cell Biol.* **8,** 4936–4948.
21. Kametaka, S., Matsuura, A., Wada, Y. & Ohsumi, Y. (1996) *Gene*, in press.
22. Klionsky, D. J. & Emr, S. D. (1989) *EMBO J.* **8,** 2241–2250.
23. Guthrie, C. & Fink, G. R. (1991) in *Guide to Yeast Genetics and Molecular Biology*, eds. Abelson, J. N. & Simon, M. I. (Academic, New York), Vol. 194, pp. 1–905.
24. Munn, A. L. & Reizman, H. (1994) *J. Cell Biol.* **127,** 373–386.